The Canadian Mineralogist
Vol. 37, pp. 1007-1023 (1999)

TOURMALINE COMPOSITIONS FROM THE SALIKVAN PORPHYRY Cu–Mo DEPOSIT AND VICINITY, NORTHEASTERN TURKEY

FUAT YAVUZ[1]

İstanbul Teknik Üniversitesi, Maden Fakültesi, Maden Yataklari-Jeokimya Anabilim Dali, 80626, Maslak, İstanbul, Turkey

ALİ İSKENDEROĞLU

Maden Tetkik Ararma Enstitüsü, Çorlu Bölgesi, 59851, Çorlu, Tekirdag, Turkey

SHAO-YONG JIANG

Max-Planck-Institut für Chemie, Postfach 3060, 55020 Mainz, Germany and National Key Laboratory of Mineral Deposit Research, Nanjing University, Nanjing 210008, Jiangsu, China

Abstract

Tourmaline-bearing rocks occur in the Pontide volcanic island arc of northeastern Turkey, which hosts numerous small- to medium-sized Cu–Pb–Zn and Cu–Mo deposits. Weakly developed porphyry-style Cu–Mo mineralization accompanies the calc-alkaline volcano-plutonic rocks of Salikvan, in southwestern Artvin. Various types of tourmaline have been analyzed chemically, of which three main environments of formation are identified: (1) quartz–tourmaline veins, (2) tonalite porphyry and, to a lesser extent, coarse granodiorite, and (3) tourmaline-rich rocks at the contacts of coarse granodiorite and basic volcanic rocks. Electron-microprobe data indicate that the tourmaline is relatively ferrous and calcic, and shows a general trend from dravite to uvite end-members; the tourmaline at Salikvan formed by the reaction of Fe-rich hydrothermal fluids with Ca-rich amphibole and plagioclase in tonalite porphyry and granodiorite. The dominant variability in composition seems controlled by the exchange vector $CaMgO\square_{-1}Al_{-1}(OH)_{-1}$. Tourmaline in quartz–tourmaline veins has moderate Fe/(Fe + Mg) values (0.37–0.51; mean 0.43), whereas that in tonalite porphyry is rich in iron, with a Fe/(Fe + Mg) of 0.45–0.53 (mean 0.48). Tourmaline in tourmaline-rich rocks is relatively rich in magnesium, with a Fe/(Fe + Mg) of 0.30–0.46 (mean 0.39). Trace-element contents of the tourmalines are low relative to those in tourmaline from massive sulfide deposits. Tourmaline has a tendency to scavenge trace elements during crystallization, yielding correlations among Ag – (Au, Li, Mo, P, Pb, Sb, V, W), Au – (P, Pb, Sb, V, W), Li – (P, Pb, Sb, V, W), Mo – (Pb, Sb, V), P – (Sb, V, W), Sb – (V, W), Co – (Cr, Mn), Pb – (Sb, V), Ba–Sr, Zn–Cu, V–W, and Cr–Mn. Chondrite-normalized patterns of the rare-earth elements point out the possible contribution of hydrothermal processes to tourmaline formation. Boron isotope analyses of tourmaline from quartz–tourmaline veins and tourmaline from tourmaline-rich rocks have $\delta^{11}B$ values of –9.4 and –9.0‰, respectively, consistent with late-magmatic hydrothermal fluids.

Keywords: tourmaline, porphyry Cu–Mo deposit, electron-microprobe data, trace elements, rare-earth elements, boron isotope, Pontide belt, Turkey.

Sommaire

Nous décrivons des roches à tourmaline provenant de l'arc insulaire des Pontides, dans le secteur nord-est de la Turquie, hôtes de plusieurs petits ou moyens gisements de type Cu–Pb–Zn et Cu–Mo. Une faible minéralisation à Cu–Mo de type porphyre accompagne les roches volcano-plutoniques calco-alcalines de Salikvan, dans le sud-ouest de la région d'Artvin. Nous avons analysé plusieurs variétés de tourmaline, dont trois principales: (1) veines à quartz–tourmaline, (2) tonalite porphyrique et, de moindre importance, granodiorite à grains grossiers, et (3) roches enrichies en tourmaline au contact de la granodiorite avec des roches volcaniques basiques. D'après les données à la microsonde électronique, la tourmaline est relativement ferreuse et calcique, et fait preuve d'une évolution générale allant de dravite à uvite; la tourmaline de Salikvan se serait formée par la réaction de fluides porteurs de Fe avec l'amphibole calcique et le plagioclase de la tonalite et de la granodiorite. La substitution prédominante semble être régie par le vecteur d'échange $CaMgO\square_{-1}Al_{-1}(OH)_{-1}$. La tourmaline des veines à quartz–tourmaline possède une valeur moyenne de Fe/(Fe + Mg) (0.37–0.51; en moyenne, 0.43), tandis que celle de la tonalite porphyrique est plus riche en fer, avec Fe/(Fe + Mg) dans l'intervalle 0.45–0.53 (en moyenne, 0.48). La tourmaline des roches enrichies en tourmaline est plutôt magnésienne, avec Fe/(Fe + Mg) dans l'intervalle 0.30–0.46 (en moyenne, 0.39). Les teneurs en éléments traces sont faibles en

[1] *E-mail address*: yavuz@sariyer.cc.itu.edu.tr

comparaison de la tourmaline des gisements de sulfures massifs. La tourmaline a tendance à concentrer les éléments traces au cours de la cristallisation, ce qui mène aux corrélations suivantes: Ag – (Au, Li, Mo, P, Pb, Sb, V, W), Au – (P, Pb, Sb, V, W), Li – (P, Pb, Sb, V, W), Mo – (Pb, Sb, V), P – (Sb, V, W), Sb – (V, W), Co – (Cr, Mn), Pb – (Sb, V), Ba–Sr, Zn–Cu, V–W, et Cr–Mn. La teneur en terres rares, par rapport au modèle chondritique, fait penser à une contribution possible de processus hydrothermaux pour expliquer la formation de la tourmaline. L'analyse des isotopes du bore dans la tourmaline de veines à quartz–tourmaline et de roches enrichies en tourmaline a donné des valeurs de $\delta^{11}B$ de –9.4 et –9.0‰, respectivement, indication supplémentaire d'une phase fluide tardi-magmatique.

(Traduit par la Rédaction)

Mots-clés: tourmaline, gisement à Cu–Mo de type porphyre, données de microsonde électronique, éléments traces, terres rares, isotopes de bore, ceinture des Pontides, Turquie.

Introduction

Tourmaline is a complex borosilicate mineral commonly found as an accessory phase in a variety of rocks and ore deposits. Its occurrence in granite-related deposits has been divided into six categories by Slack (1996): (1) Sn ± W greisens, veins, skarns, and replacements, (2) Cu ± Au breccia pipes and Cu ± Mo porphyries, (3) Au-bearing veins, (4) Cu-bearing veins and replacements, (5) U-bearing veins, and (6) Pb–Zn veins and replacements. Studies of granite-related porphyry systems have focussed on Sn, W, Cu, and Mo associations (Sillitoe 1973, Patterson *et al.* 1981, Warnaars *et al.* 1985, Pirajno *et al.* 1987, Lynch 1989, Wright & Kwak 1989, Layne & Spooner 1991, Koval *et al.* 1991, Pirajno & Smithies 1992, Lubis *et al.* 1994, London & Manning 1995, Lynch & Ortega 1997). We focus here on tourmaline in the Salikvan porphyry Cu–Mo deposit.

The northern metallogenic belt of Turkey, also called the Pontide belt, represents a volcanic island-arc system that contains many small- to medium-sized polymetallic (Cu – Pb – Zn ± Ag ± Au) sulfide deposits. Within this belt, numerous small porphyry copper deposits are hosted by volcano-plutonic rocks of Cretaceous to Paleogene age. The weakly mineralized Salikvan porphyry Cu–Mo deposit is part of the Balkan – Caucasus – Iran Cu–Mo belt, and constitutes its northeastern extension in Turkey. Mineralization shows similar characteristics to the Balcılı Cu–Mo occurrences (Yavuz 1992), located in the southeastern part of the study area, except for its porphyritic groundmass and tourmaline content. Field studies indicate that the Salikvan area represents the upper part of the Balcılı Cu–Mo mineralized system.

Tourmaline chemistry plays an important role in constraining the genesis of hydrothermal deposits in granite-related porphyry systems. In most porphyry Cu–Mo systems, the tourmaline is rich in ferric iron, with compositions ranging from dravitic to schorl end-members. Tourmaline from the Salikvan area, however, shows a dominantly dravitic composition and, to a lesser extent, an enrichment in the uvite component. In this paper, we describe recently discovered occurrences of tourmaline in the Salikvan porphyry Cu–Mo deposit, document its chemical composition, and speculate on the use of some trace elements in tourmaline as an exploration guide for porphyry Cu–Mo deposits without breccia pipe associations. A regression analysis of the trace-element contents of tourmaline from the Salikvan Cu–Mo deposit shows that Li – (Ag, P, Pb, Sb, V, W), P – (Ag, Au, Li), Pb – (Ag, Au, Li, Mo, Sb, V), Sb – (Ag, Au, Li, Mo, Pb), V – (Ag, Au, Li, Mo, Pb, W), W – (Ag, Au, Li, V), Mn – (Co, Cr), Sr – (Ba), and Sn – (Zr) can be used as indicator elements in defining the characteristics of mineralization and the processes of hydrothermal alteration in the Salikvan deposit.

Geological Setting

The Pontide metallogenic belt in northern Turkey lies within the Black Sea region and hosts a number of ore deposits related to Upper Cretaceous calc-alkaline volcanic rocks, which are generally dacitic in composition. In the eastern Pontide island arc environment, several types of mineral deposits are present. These include: (1) massive sulfide deposits (Cu–Zn–Pb), (2) skarn-type deposits (Fe, Fe–Cu), (3) vein-type deposits (Pb, Pb–Zn, Cu–Zn), and (4) porphyry-type deposits (Cu, Cu–Mo). The oldest unit in the eastern Pontide belt consists of pre-Paleozoic metamorphic rocks. These rocks are unconformably overlain by Jurassic spilitic basalts and keratophyric andesites, which are called the lower basic series. This series is overlain by Upper Cretaceous units including ore-bearing dacites, their pyroclastic equivalents, basalts, and a volcano-sedimentary series. All these units are intruded by later granitic rocks, up to Tertiary age. Skarn-type deposits are present arround the contacts of granitic rocks. Ore-bearing dacites of Upper Cretaceous age are host to many massive sulfide deposits. Vein-type deposits are widespread in the eastern Pontide metallogenic belt. Porphyry Cu–Mo deposits are generally developed at the border and apex of granitic plutons (Aslaner *et al.* 1995).

The Salikvan area is located in the northeastern part of the Black Sea region, about 50 km southwest of Artvin (Fig. 1). The study area is composed of felsic to intermediate intrusive rocks of Upper Cretaceous to Tertiary age; these make up the border zone of the Rize

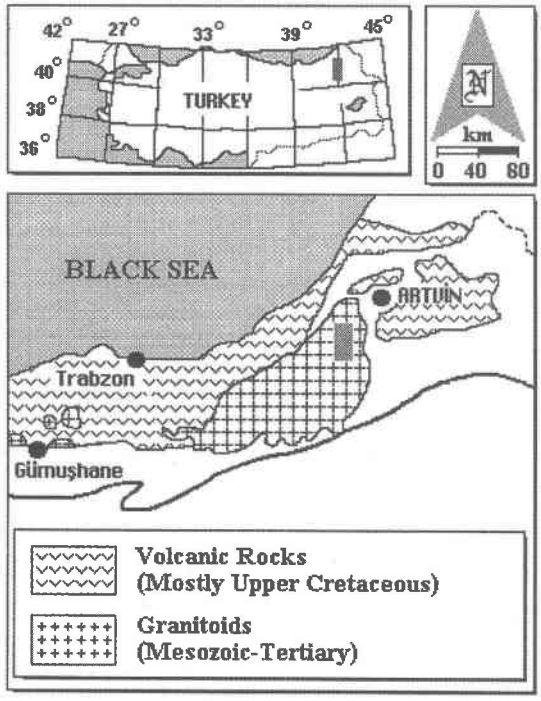

FIG. 1. Map showing location of the Salikvan porphyry Cu–Mo deposits (shaded rectangle) within the northeast Black Sea region of Turkey.

batholith. Moore *et al.* (1986) obtained a K–Ar age of 62.4 ± 4.2 Ma for the Balcılı granodiorite exposed southeast of the study area. In this paper, we present new high-analytical-precision K–Ar data on biotite from the Balcılı granodiorite. The K–Ar isotope data correspond to 64.5 ± 1.7 Ma, as determined by Geochron Laboratories, Acton, Massachusetts. The Salikvan porphyry constitutes the upper part of this intrusive unit.

The geology of the area (Fig. 2) was first investigated by geologists of the Institute of Mineral Research and Exploration (Kahraman *et al.* 1987), but was examined in detail for this study. The oldest unit in the area is Lower Cretaceous and comprises andesitic and basaltic lavas and related pyroclastic units of the lower basic series. The lower basic series is characterized by pale and dark green colors in outcrops. Depending on the degree of alteration, the indicators of alteration include quartz, calcite, white mica, chlorite, and pyrite. Upper Cretaceous dacitic, andesitic and basaltic lavas and associated tuffs and pyroclastic rocks overlie this series. Most of the polymetallic mineralization in the eastern Pontide accompanies dacitic rocks. Intense hydrothermal alteration is observed in these rocks. The major-element geochemistry of the Upper Cretaceous magmatic rocks indicates I-type features. Their multi-element chondrite-normalized spectra yield patterns similar to those of normal subduction-related granites (Yavuz & Bürküt 1993, Tokel 1995). All parts of this unit are cut by younger granites, which are grouped into five categories: coarse granodiorite, microgranodiorite, monzodiorite, tonalite porphyry, and Balcılı granodiorite. The coarse granodiorite, typically medium to coarse grained, is associated with tourmaline-rich rocks at the contact of the lower basic series. The concentration of tourmaline increases from the coarse granodiorite to the lower basic series and reaches nearly parallel bands up to 5 cm thick intercalated with the lower basic series. Tourmaline occurrences are dominant in the tonalite porphyry, both as anhedral to subhedral grains and as euhedral grains in quartz veins; these veins cut the coarse granodiorite, tonalite porphyry and monzodiorite. The tourmaline in the quartz veins is generally observed as needle-like and prismatic euhedral to subhedral crystals up to 3 cm long.

PETROGRAPHY

Three modes of tourmaline occurrence have been established in the Salikvan porphyry Cu–Mo deposit. The first comprises medium- to fine-grained prismatic tourmaline (0.5 mm – 3.0 cm) in quartz–tourmaline veins, the width of the crystals attaining 2.0 mm. Widespread euhedral chlorapatite accompanies the tourmaline (Fig. 3A). This type of tourmaline typically shows concentric color-zonation, with a light bluish green core and a deep green to brown rim under crossed nicols (Fig. 3B). Reverse color-zonation has also been observed locally in some of the vein-hosted tourmaline. The second mode of occurrence is most common in tonalite porphyry. The tourmaline in this case is in general unzoned, but color zonation without major-element variation is present in some anhedral crystals. Well-developed microscopic tourmaline suns are encountered in the matrix of the tonalite porphyry (Fig. 3C). In amphibole-bearing tonalite porphyry, tourmaline occurs as disseminated anhedral to subhedral grains and shows brown and bluish green pleochroism (Fig. 3D). Replacement of amphibole by tourmaline was observed in some cases. Microscopic needles of tourmaline occur as fracture fillings in tonalite porphyry, with blue to colorless pleochroism (Fig. 3E). Secondary tourmaline also is present in tonalite porphyry in association with chlorite in the core of altered plagioclase. Tourmaline in this type of occurrence was developed at the expense of plagioclase. The compositions of tourmaline change slightly in terms of magnesium content toward the north side of the study area, where tourmaline-rich rock is encountered between the contact between the lower basic series and coarse granodiorite. In the third mode of occurrence, tourmaline forms small crystals and is associated with pyrite and magnetite. Late-stage tourmaline developed in fractured tonalite porphyry contains inclusions of subhedral to euhedral zircon and apatite (Fig. 3F).

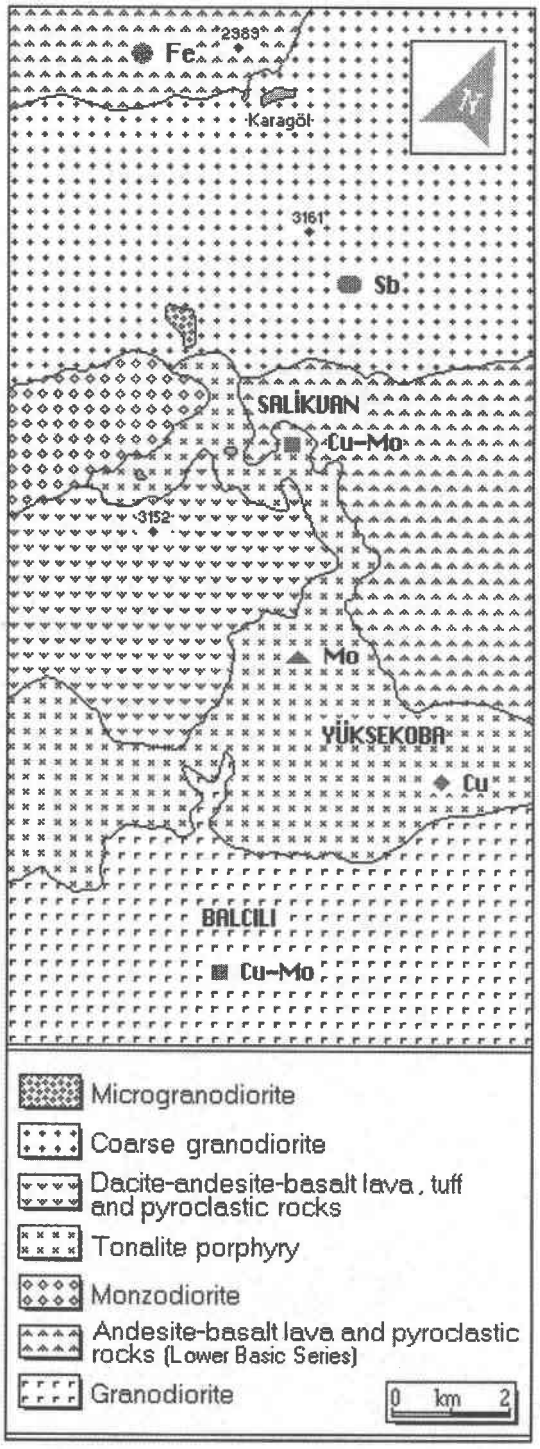

FIG. 2. Geological sketch-map of the Salikvan porphyry Cu–Mo deposit and vicinity. Other metal deposits and occurrences also are shown.

HYDROTHERMAL ALTERATION AND MINERALIZATION

Tourmaline in porphyry Cu ± Mo mineralized systems is most abundant in granite-related breccia pipes (*e.g.*, Chile: Sillitoe & Sawkins 1971), and is less common in non-breccia associations (*e.g.*, Bajan–Ula, Russia: Koval *et al.* 1991). Tourmaline in non-breccia associations typically is concentrated in white-mica-rich alteration zones (*e.g.*, El Teniente, Chile: Camus 1975), but in some porphyry Cu–Mo deposits, it occurs in zones of Na–Ca or K-feldspar alteration (*e.g.*, Yerington, Nevada: Carten 1986). A detailed listing of tourmaline-bearing breccia pipes and porphyry deposits was given by Slack (1996).

Numerous polymetallic and Cu–Mo anomalous areas in northern Turkey were defined within the context of a cooperative geochemical project between the United Nations and the Mineral Research and Exploration (MTA) in 1975. Kamitani & Takaoğlu (1976) later studied the areas of Cu–Mo anomaly. The Salikvan Cu–Mo anomaly, which outcrops 10 km northwest of the Balcılı deposit, was investigated in detail in this study. On the basis of detailed field, microscopic, and geochemical studies, Yavuz (1992) distinguished three zones of alteration in the Balcılı area (potassic, phyllic, and propylitic), with insignificant copper and molybdenum mineralization. Electron-microprobe data on hydrothermal biotite (unpubl. data) from the Balcılı porphyry Cu–Mo mineralization area give a mean of 390°C for the development of potassic alteration zone using the BIOTERM software (Yavuz & Öztaş 1997). Potassic, phyllic, propylitic, and late-stage sodic alteration zones also were observed in the Salikvan deposit and surrounding rocks (Fig. 4). The weakly developed zone of potassic alteration is characterized by fine-grained biotite + quartz + chalcopyrite + pyrite ± molybdenite. In the phyllic alteration zone, white mica + quartz + chlorite + pyrite ± chalcopyrite constitutes the main mineral assemblage. Propylitic alteration led to the assemblage epidote + calcite + chlorite ± albite ± pyrite ± chalcopyrite. In this zone, albite formed by release of calcium from calcium-rich plagioclase. Late-stage sodic alteration, developed at shallow depths, is characterized by an albite + tourmaline assemblage that is superimposed on the propylitic assemblage. Tourmaline is generally absent in the potassic and phyllic alteration zones, but is widespread in the sodic alteration zone, where tonalite porphyry constitutes the main rock-type. Pyrite is the dominant sulfide mineral in association with chalcopyrite ± molybdenite in quartz veins and quartz veinlets in the groundmass of the porphyry. Quartz veins up to 20 cm thick contain the assemblage pyrite + chalcopyrite ± stibnite ± molybdenite; they are generally located along northeast–southwest-trending and north-dipping tensional fissures (Kamitani *et al.* 1977). The copper and molybdenum contents of samples taken from the Salikvan and surrounding mineralized area range from 0.3 to 1.5% and 0.07 to 0.15%, respectively (Yavuz 1992, Kahraman *et al.* 1987).

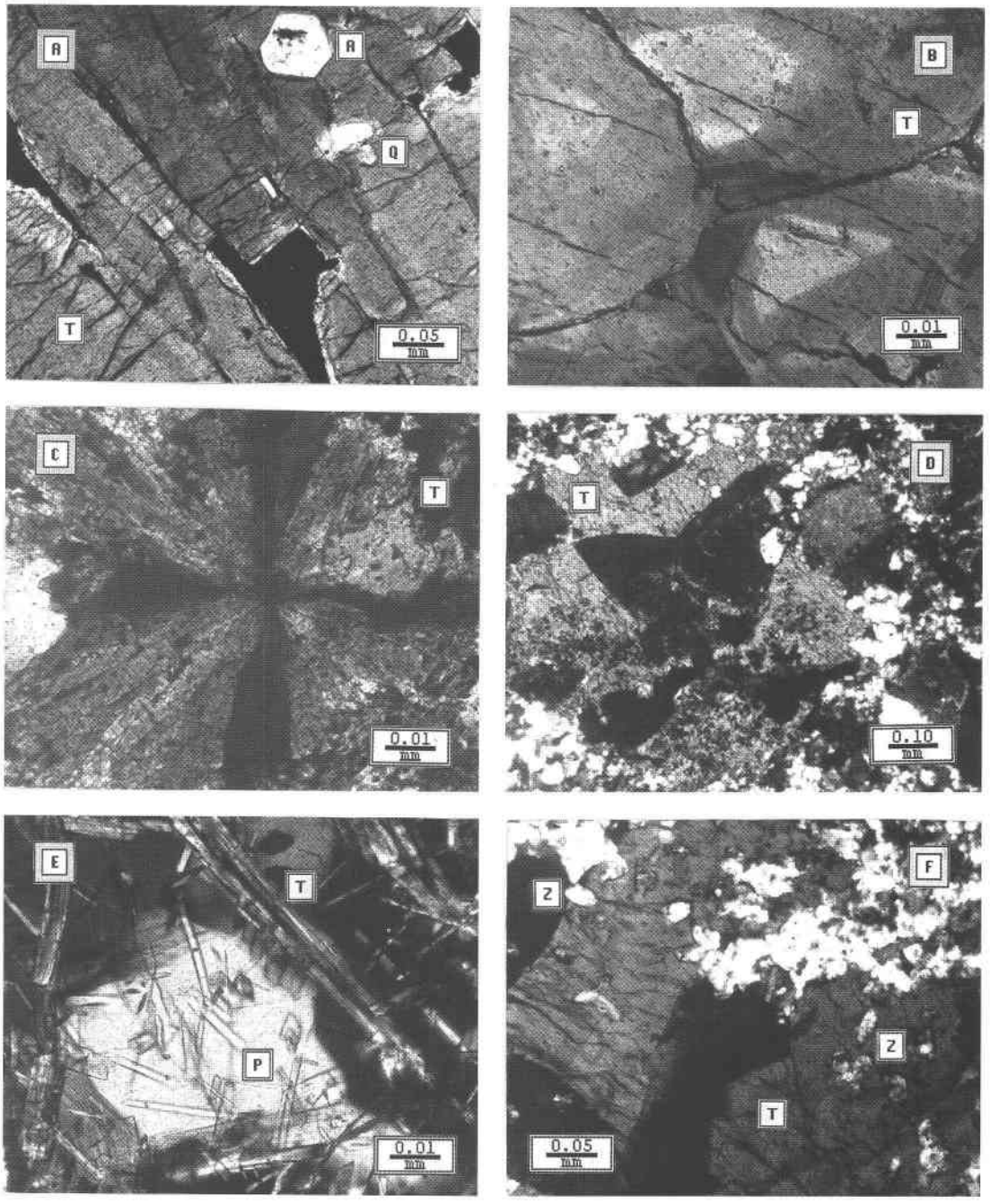

FIG. 3. Photomicrographs (crossed polars). A. Euhedral crystals of tourmaline (T) associated with apatite (A) and quartz (Q). B. *C*-axis section of zoned tourmaline (T) in quartz–tourmaline vein. C. Well-developed tourmaline sun (T) in tonalite porphyry together with quartz (Q). D. Anhedral to subhedral tourmaline (T) in tonalite porphyry. E. Tourmaline needles (T) developed in association with albite (P) in coarse granodiorite. F. Apatite and zircon inclusions in tourmaline crystals.

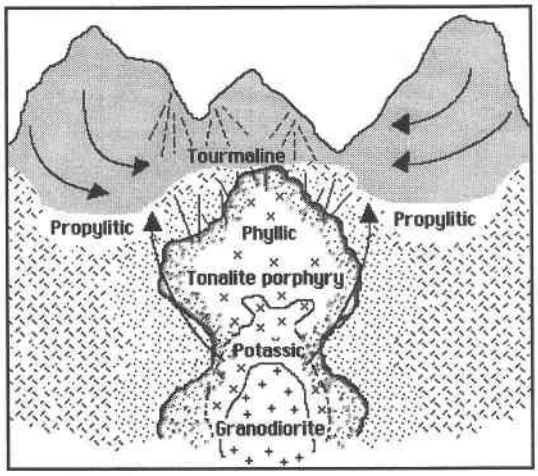

FIG. 4. Generalized diagram showing the tourmalinization and alteration zones in the Salikvan porphyry Cu–Mo deposit.

COMPOSITION OF THE TOURMALINE

Sampling and analytical methods

A total of 20 samples were collected from the study area. They were selected from representative quartz–tourmaline veins, tourmaline-rich rocks, and tourmaline-bearing magmatic rocks. Tourmaline separates were hand-picked with a binocular microscope to remove other mineral grains, and then ground in an agate mortar for chemical analysis. The trace- and rare-earth-element (*REE*) contents of the tourmaline samples were carried out by a commercial laboratory in Canada using ICP–AES and INAA techniques.

Chemical analyses of the tourmalines were done at the Şişecam Research Center in İstanbul using an automated JEOL 733 electron microprobe operated at a voltage of 15 kV, a beam current of 15 nA, a beam diameter of 5 μm, 30 s counting times, and a ZAF correction scheme. Natural minerals and synthetic compounds were used as standards. Compositions of tourmaline were obtained on 21 grains in six polished thin sections. Representative electron-microprobe data are listed in Table 1, with unit formula calculated on the basis of 24.5 anions. Boron contents were assumed to total 3 B atoms per formula unit, *apfu*. The TOURMAL computer program of Yavuz (1997) was used for calculations and for plotting of the chemical data.

Major elements

The general formula of tourmaline is given as $XY_3Z_6Si_6O_{18}(BO_3)\ W_4$, where $X = Na^+, Ca^{2+}, K^+$, or vacancy; $Y = Mg^{2+}, Fe^{2+}, Mn^{2+}, Al^{3+}, Fe^{3+}, Mn^{3+}, Li^+$; $Z = Al^{3+}, Mg^{2+}, Fe^{3+}, Cr^{3+}, V^{3+}$, and $W = O^{2-}, OH^-, F^-, Cl^-$. In general, schorl (Na–Fe^{2+}) and elbaite (Al–Li) constitute the main end-members in granitic rocks and their associated aplites and pegmatites, whereas tourmaline associated with massive sulfide deposits generally tends toward dravitic (Na–Mg) compositions (Slack 1996). Compositions intermediate between dravite and schorl are observed in tourmaline from many sedimentary and metamorphic rocks (Henry & Guidotti 1985, Henry & Dutrow 1990).

The tourmaline samples range from 5.82 to 12.69 wt% FeO, 6.32 to 8.18% MgO, 0.33 to 2.02% TiO_2, 1.02 to 2.59% CaO, 1.01 to 2.09% Na_2O, and 25.12 to 30.55% Al_2O_3. Contents of Mn are negligible (< 0.09% MnO). Mg values are generally uniform at close to 1.80 *apfu*. Si is commonly 6 atoms per formula unit (*apfu*). There is no major variation in Al content, but Fe varies

TABLE 1. REPRESENTATIVE COMPOSITIONS OF TOURMALINE FROM THE SALIKVAN PORPHYRY Cu–Mo DEPOSIT

	1	2	3	4	5	6	7	8	9	10
SiO_2 (wt%)	35.67	36.68	36.12	35.47	36.70	35.80	35.29	37.56	38.52	35.98
Al_2O_3	27.56	28.59	29.19	25.12	29.06	26.43	28.41	30.55	30.43	26.78
TiO_2	1.48	0.50	0.60	1.89	0.48	1.01	0.73	0.49	0.58	1.65
FeO*	9.78	8.41	9.38	12.29	9.68	12.69	10.26	5.82	7.05	9.61
MgO	6.99	6.81	7.01	6.71	6.54	6.32	6.96	7.57	7.46	7.45
CaO	2.20	1.78	1.74	2.31	1.70	2.44	1.84	1.24	1.13	2.59
Na_2O	1.80	2.05	1.98	1.26	1.32	1.54	1.92	1.01	1.39	1.01
K_2O	0.00	0.09	0.00	0.00	0.00	0.00	0.00	0.00	0.09	0.00
Total	85.48	84.91	86.02	85.05	85.48	86.23	85.41	84.24	86.65	85.07
Structural formulae on the basis of 24.5 atoms										
B *apfu*	3.00	3.00	3.00	3.00	3.00	3.00	3.00	3.00	3.00	3.00
Si	6.03	6.16	6.03	6.11	6.14	6.09	5.98	6.20	6.24	6.09
Al_T	0.00	0.00	0.00	0.00	0.00	0.00	0.02	0.00	0.00	0.00
ΣT	6.00	6.00	6.00	6.00	6.00	6.00	6.00	6.00	6.00	6.00
Al_Z	5.49	5.66	5.74	5.10	5.73	5.30	5.65	5.94	5.81	5.34
Fe^{3+}	0.51	0.34	0.26	0.90	0.27	0.70	0.35	0.06	0.19	0.66
ΣZ	6.00	6.00	6.00	6.00	6.00	6.00	6.00	6.00	6.00	6.00
Al_Y	0.00	0.00	0.00	0.00	0.00	0.00	0.00	0.00	0.00	0.00
Ti	0.19	0.06	0.08	0.24	0.06	0.13	0.09	0.06	0.07	0.21
Fe^{2+}	0.87	0.84	1.05	0.87	1.08	1.11	1.10	0.74	0.76	0.70
Mg	1.76	1.71	1.74	1.72	1.63	1.60	1.76	1.86	1.80	1.88
ΣY	2.82	2.61	2.87	2.83	2.77	2.84	2.95	2.66	2.63	2.79
Ca	0.40	0.32	0.31	0.43	0.30	0.44	0.33	0.22	0.20	0.47
Na	0.59	0.67	0.64	0.42	0.43	0.51	0.63	0.32	0.44	0.33
K	0.00	0.01	0.00	0.00	0.00	0.00	0.00	0.00	0.01	0.00
ΣX	0.99	1.00	0.95	0.85	0.73	0.95	0.99	0.54	0.65	0.80
Σ Cations	15.84	15.77	15.85	15.79	15.64	15.88	15.94	15.40	15.52	15.68
R1 + R2	4.13	3.88	4.00	4.34	3.72	4.36	4.17	3.24	3.39	4.05
R3	5.74	5.75	5.84	5.43	5.81	5.47	5.79	6.02	5.90	5.62
$Fe^{2+}/(Fe^{2+}+Fe^{3+})$	0.63	0.71	0.80	0.49	0.80	0.61	0.76	0.93	0.80	0.51
$Fe^{2+}/(Fe^{2+} + Mg)$	0.33	0.33	0.38	0.34	0.40	0.41	0.38	0.28	0.30	0.27
Mg/(Mg + Fe)	0.56	0.59	0.57	0.49	0.55	0.47	0.55	0.70	0.65	0.58
Na/(Na + Ca)	0.60	0.68	0.67	0.50	0.58	0.53	0.65	0.60	0.69	0.41

Samples 1, 2, 3, 4: tourmaline in quartz–tourmaline veins; 5, 6, 7: tourmaline in tonalite porphyry; 8, 9, 10: tourmaline in tourmaline-rich rocks. R1 = Na + Ca; R2 = Fe + Mg + Mn; R3 = Al + 1.33*Ti. *Total iron as FeO. Electron-microprobe data; *apfu*: atoms per formula unit.

between 0.80 and 1.81 *apfu*. In all cases, FeO contents are greater than MgO; most show CaO exceeding Na_2O. Tourmaline from the Salikvan area is generally ferrous and calcic (dominant dravite and, to a lesser extent, uvite, and displays a general trend toward ferric components. On an Al–Fe–Mg diagram (Henry & Guidotti 1985), the tourmaline compositions plot in field of 5 and 6 (Fig. 5), which correspond to tourmaline from metapelites and metapsammites not coexisting with an Al-saturating phase (field 5) and Fe-rich quartz–tourmaline rocks, calc-silicate rocks, and metapelites (field 6). The mean composition of tourmaline from Salikvan and other porphyry-type systems is shown for comparison in Figure 5. Tourmaline from the investigated area is compositionally similar to that from Chilean porphyry copper deposits.

Trace elements

The composition of tourmaline is useful in geochemical exploration; toumaline-group minerals crystallize during late stages of magmatic evolution and scavenge trace elements from their environment of formation. In recent years, many studies have focussed on the trace-element content of tourmaline in igneous and hydrothermal environments. Kitayev & Bogatyrev (1984) used elevated Au, Ag, As, Bi, and Mo values in tourmaline from quartz–tourmaline mineralization in gold deposits as a prospecting tool. Smith *et al.* (1987) used emission spectroscopic data derived from hydrothermal tourmaline from northern Mexico. Gorelikova & Naumova (1987) presented trace-element data in tourmaline associated with tin deposits in Siberia to identify levels of mineralization. Geochemical characteristics of tourmaline from Archean lode-gold deposits in the Superior Province of Ontario were given by King (1988), based on ICP and XRF methods combined with a modified INAA technique. Koval *et al.* (1991) used atomic absorption and emission spectroscopic methods to characterize tourmaline from gold-bearing quartz veins and porphyry Cu–Mo deposits in Russia. The concentrations of trace elements, including the rare-earth elements, were determined by the ICP–MS technique by Jiang & Palmer (1995) in tourmaline from granite-related Sn and stratiform Pb–Zn–Ag deposits. Mittwede *et al.* (1995a, b) reported some trace-element contents in tourmaline and tourmalinite from the area of Lake Bafa, southeastern Anatolia, and in quartz–tourmaline nodules from Irmadan (Muğla-Yatağan), Turkey.

Trace-element abundances of pure tourmaline concentrates from the Salikvan porphyry Cu–Mo deposit were established by inductively coupled plasma – atomic emission spectroscopy (ICP–AES) for Cu, Pb, Zn, Mn, Ag, Bi, Cd, Ni, Co, Sr, V, P, Cr, Ba, Zr, Sn, Sc, Nb, and Li. Concentrations of Mo, As, Au, Sb, W, U, Th, Hf, Cs, Se, and Rb were established by instrumental neutron-activation analysis (INAA). A commercial laboratory carried out both ICP–AES and INAA analyses (Table 2). Trace-element results for Cu, As, Ni, V, Zr, Sn, and Li in tourmaline from quartz–tourmaline veins and tourmalinite are similar. Small variations exist for Pb (8–39 ppm), Zn (19–76 ppm), Ag (0.5–1.3 ppm), Co (2–11 ppm), Au (8.1–107.5 ppb), Sr (97–177 ppm), Sb (1.6–36.9 ppm), Cr (4–14 ppm), Ba (18–60 ppm), W (1–16 ppm), Sc (15–29 ppm), P (40–80 ppm), and Mn (194–262 ppm). Contents of some elements are below detection limits, for example U (< 0.5 ppm), Th (< 0.2 ppm), Nb (< 2 ppm), Be (< 1 ppm), Cd (< 1 ppm), Cs (< 1 ppm), Hf (< 1 ppm), Rb (< 15 ppm), and Se (< 3 ppm), and are not shown in Table 2.

TABLE 2. TRACE-ELEMENT CONCENTRATIONS IN TOURMALINE AND GRANITIC ROCKS FROM THE SALIKVAN PORPHYRY Cu–Mo DEPOSIT

	T1	T2	T3	T4	T5	R1	R2
Cu ppm	3	4	3	3	4	21	16
Pb	39	35	8	10	25	30	14
Zn	22	76	19	25	53	53	92
Mo	3.36	5.07	2.63	2.03	4.45	6	5
Au*	107.5	152.1	10.5	8.1	39.6	n.a.	n.a.
Ag	1.3	1	0.5	0.3	0.7	0.5	0.5
Mn	194	180	262	250	223	553	1404
Ni	<2	<2	4	<2	3	13	5
Co	2	3	7	11	8	5	7
As	<1	15.20	<1	<1	<1	3	9
P	80	50	40	20	30	n.a.	n.a.
Sb	36.96	34.98	2.62	1.62	23.14	3.8	1.3
Bi	5	<5	<5	<5	<5	<5	6
V	164	163	161	161	162	70	76
Cr	5	4	11	14	10	12	34
W	43.68	50.70	41.84	24.30	26.70	6	4
Zr	2	3	3	2	2	6	5
Sn	4	5	5	3	3	<2	<2
Sc	28	29	3	26	21	6	10
Sr	177	105	97	148	163	532	360
Ba	60	23	18	36	52	658	621
Li	9	6	5	5	6	n.a.	n.a.

Samples T1, T2: tourmaline in quartz–tourmaline veins; T3, T4, T5: tourmaline in tourmaline-rich rock; R1: coarse granodiorite; R2: tonalite porphyry. *: ppb; n.a.: not analyzed).

Tourmaline from quartz–tourmaline veins has higher Pb, Zn, Ag, Sr, Sb, Ba, W, P, Sn, Li, and Au, but lower Ni, Co, Mn, Cr, and Zr contents than that from the tourmaline-rich rock. The concentrations of Cu and V lack systematic variations both in tourmaline-rich rock and in quartz–tourmaline veins. Concentrations of Ni, Co, Mn, and Cr in tourmaline-rich rocks, which are locally widespread along the contacts of lower basic series and coarse granodiorite, are considerably higher than in tourmaline from the quartz–tourmaline veins. Widespread euhedral crystals of chlorapatite occur in the quartz–tourmaline veins and hence, amounts of P in this type of rock are higher than in the occurrences of tourmaline-rich rock.

Base-metal contents of tourmaline generally reflect its associated sulfide mineralization. Griffin *et al.* (1996) plotted data for Cu, Pb, and Zn in tourmaline samples from many massive sulfide deposits on a triangular dia-

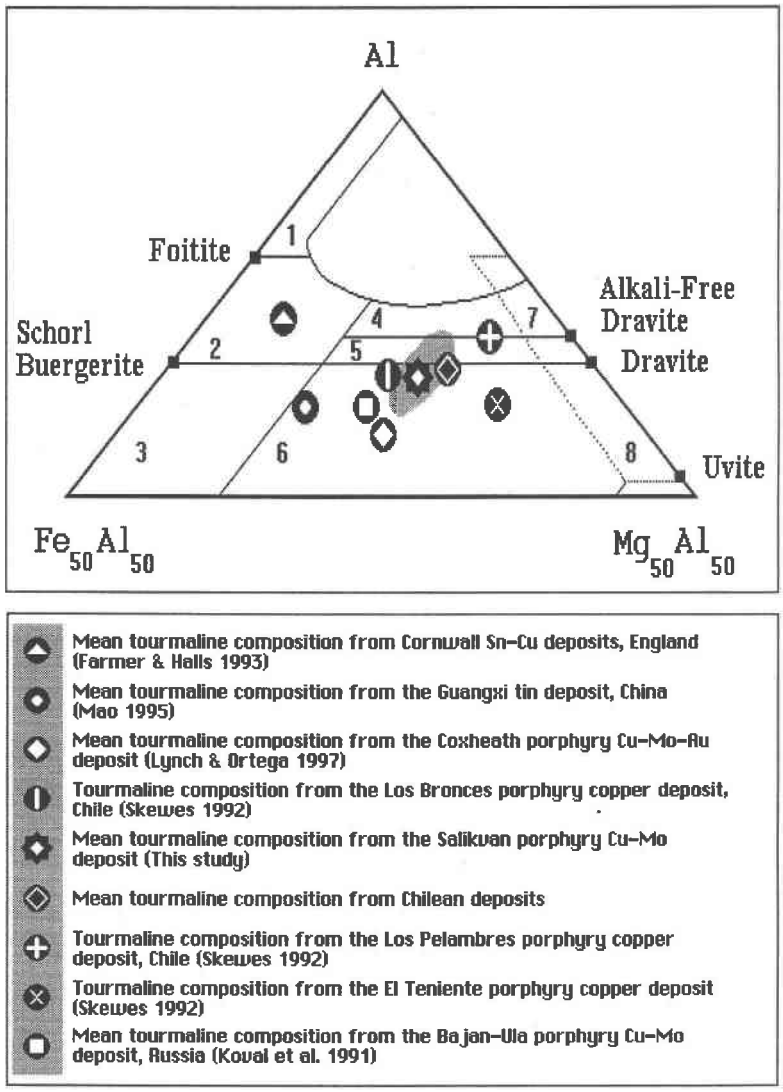

FIG. 5. Plot of the tourmaline compositions at Salikvan (shaded area) in terms of Al–Fe–Mg, together with mean composition of tourmaline in other hydrothermal systems. All data, except for the mean composition from the Los Pelambres porphyry copper deposit in Chile and from hydrothermal veins in the Cornwall (England) district lie below the schorl–dravite line (*i.e.*, in the field of Fe^{3+}-bearing tourmalines). The numbered fields (after Henry & Guidotti 1985) correspond to: (1) Li-rich granitic rocks and their associated pegmatites and aplites, (2) Li-poor granitic rocks and their associated pegmatites and aplites, (3) Fe^{3+}-rich quartz–tourmaline rocks (hydrothermally altered granites), (4) metapelites and metapsammites coexisting with an Al-saturating phase, (5) metapelites and metapsammites not coexisting with an Al-saturating phase, (6) Fe^{3+}-rich quartz–tourmaline rocks, calc-silicate rocks and metapelites, (7) low-Ca metaultramafic rocks and Cr,V-rich metasedimentary rocks, and (8) metacarbonates and metapyroxenites.

gram. Samples of tourmaline from the Salikvan area plot in the middle of the diagram, close to the Cu–Zn join (Fig. 6A). On an Ag–Au–Sb diagram, the data points define a narrow range parallel to the Ag–Sb join and close to the Sb apex (Fig. 6A). Limited data are available for trace-element contents of tourmaline from porphyry copper environments. The compositions of tourmaline from the Salikvan porphyry Cu–Mo deposit are plotted on a Sn–Mo–Cu diagram (Fig. 6B) together with the average compositions of tourmaline from the Bajan–Ula porphyry Cu–Mo occurrence in Russia (Koval *et al.* 1991). The concentration of tin in tourmaline from the Salikvan area seems to be higher than in that from the Bajan–Ula area. Trace-element contents of tourmaline from the Salikvan deposit indicate that molybdenum concentration cannot be correlated directly with the degree of enrichment of the associated sulfide mineralization. This finding is also supported by the mean composition of tourmaline from the Bajan–Ula porphyry Cu–Mo deposit, which in terms of W–Mo–Sn proportions lies toward the W apex (Fig. 6B). Chemical compositions of the tourmalinites, in terms of Na, Ca, K, Sr, Ba, and Zn/(Zn + Pb), are different from those of tourmaline in the quartz–tourmaline veins. Tourmaline in the tourmaline-rich rock has higher K, Zn/(Zn + Pb), and lower Na, Ca, Ba, and Sr values than the vein tourmaline.

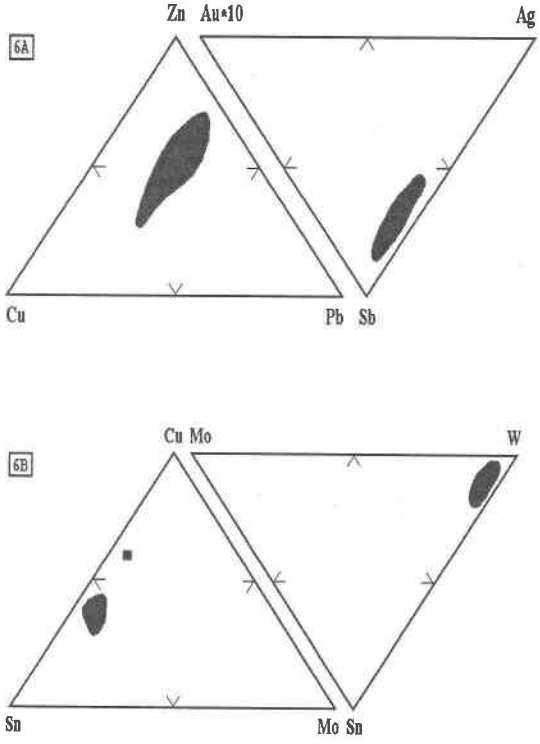

FIG. 6. Trace-element concentrations in tourmaline. A. Cu–Pb–Zn and Ag–Au*10–Sb. B. Sn–Mo–Cu and W–Mo–Sn. Filled-square symbol in Figure 6B refers to the composition of tourmaline from the Bajan–Ula porphyry Cu–Mo deposits in Russia (Koval *et al.* 1991).

Rare-earth elements

The rare-earth-element content of tourmaline provides important constraints for assessing its genesis. Studies of the *REE* abundances of tourmaline from various environments have increased in the last decade, owing in part to developments in analytical techniques (King & Kerrich 1986, King 1988, King *et al.* 1988, Slack *et al.* 1993, Hellingwerf *et al.* 1994, Garba 1996, Cleland *et al.* 1996). The *REE* concentrations in tourmaline from a quartz–tourmaline vein, a tourmaline-rich rock, and host coarse granodiorite and tonalite porphyry are given in Table 3. Data for the *REE* were obtained using the INAA technique. The determination of trace-element and *REE* abundances in tourmaline and other boron-bearing minerals by INAA is affected by suppression of the incident neutron flux in the target sample during irradiation, arising from the intrinsically large neutron-capture cross-section of boron. King *et al.* (1988) reported that the neutron-capture effect lowers the INAA-determined abundance of *REE*s in tourmaline by about 60%. Taking this effect into account, the *REE* concentrations of tourmaline samples from the quartz–tourmaline veins and the tourmaline-rich rock in Salikvan deposit are corrected using the procedure proposed by Slack *et al.* (1993) and Slack (1996). The total *REE* concentrations of the tourmaline samples are low. Their total *REE* contents range between 17.5 and 45.5 ppm.

TABLE 3. RARE-EARTH-ELEMENT CONCENTRATIONS IN TOURMALINE AND GRANITIC ROCKS FROM THE SALIKVAN PORPHYRY Cu–Mo DEPOSIT

	T1	T2	T3	T4	R1	R2
La ppm	3.36	10.14	15.69	12.15	42	26
Ce	10.08	15.21	20.92	12.15	72	50
Nd	0.34	0.51	1.05	0.81	20	18
Sm	0.34	1.01	1.57	0.81	3	4
Eu	0.34	1.01	1.05	0.40	0.7	0.9
Yb	2.69	3.55	4.18	3.24	1.2	3.4
Lu	0.34	0.51	1.05	0.81	0.5	0.56
La_N/Sm_N	6.22	6.32	6.29	9.44	8.0	4.6
La_N/Yb_N	0.84	1.93	2.54	2.53	23.64	5.17
La_N/Ce_N	0.86	1.74	1.96	2.60	1.52	1.36
Ce/Ce_N	10.53	15.89	21.86	12.69	75.23	52.25
Eu/Eu*	0.97	1.46	1.12	0.68	0.32	0.67
Sm/Nd	1.00	1.98	1.49	1.00	1.50	0.22
Sr/Eu	520.6	103.9	92.4	370.0	760.0	400.0
La/Yb	1.25	2.86	3.75	3.75	35.00	7.65
Σ *REE*	17.49	31.94	45.51	30.37	166.4	92.9

Samples T1, T2: tourmaline in tourmaline–quartz veins; T3, T4: tourmaline in tourmaline-rich rocks; R1: coarse granodiorite; R2: tonalite porphyry.

Chondrite-normalized patterns of the *REE* from the tourmaline in quartz–tourmaline veins and tourmaline from the tourmaline-rich rock are shown in Figure 7, together with the tourmaline-bearing magmatic rocks. The plot of *REE* concentrations shows a different spectrum in terms of rock types and tourmaline occurrences. Tourmaline from the quartz–tourmaline veins and tourmaline from the tourmaline-rich rocks show poorly fractionated chondrite-normalized patterns ($La_N/Yb_N = 0.84$ and 2.54, respectively), and generally decrease in light *REE* and increase in heavy *REE* (Fig. 7). The coarse granodiorite shows a highly fractionated pattern with a chondrite-normalized value of $La_N/Yb_N = 23.6$. On the other hand, the tonalite porphyry, which hosts extensive tourmalinization, has a poorly to moderately fractionated pattern, with $La_N/Yb_N = 5.2$. The tourmaline-bearing tonalite porphyry is moderately enriched in light *REE*, with normalized La_N abundances of 70–114 times chondrite and La_N/Sm_N values from 4.6 to 8.0. Tourmaline from the quartz–tourmaline veins (T1 and T2 in Table 3) is depleted in the light *REE*, with normalized La_N contents of 9.15 and 27.68 times chondrite and a La_N/Sm_N of 6.2 to 6.3, in contrast to tourmaline in the tourmaline-rich rocks (T3 and T4 in Table 3) with normalized La_N abundances of 42.8 and 33.1 times chondrite and La_N/Sm_N values between 6.3 and 9.4. The tourmaline from quartz–tourmaline veins is characterized by a small positive Eu anomaly (Eu/Eu* in the range 0.97–1.46), whereas tourmaline from tourmaline-rich rocks shows a variable Eu anomaly (Eu/Eu* in the range 0.68–1.12). Both tourmaline from quartz–tourmaline veins and that from tourmaline-rich rocks are marked by a progressive depletion from La to Sm and enrichment in the heavy *REE* (Yb, Lu) with a small positive Eu anomaly. Low total *REE* concentration, together with small positive Eu and negative Ce anomalies, suggest that the *REE* were contributed to the system by hydrothermal solutions (Klein & Beukes 1989). The chondrite-normalized *REE* pattern of tourmaline from tourmaline-rich rocks shows a trend similar to that of tourmalinite formed in submarine environments.

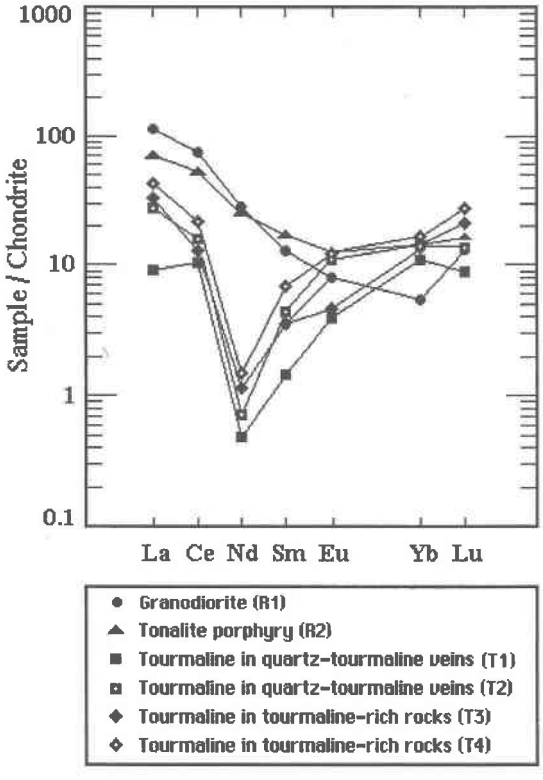

FIG. 7. Chondrite-normalized diagram showing *REE* patterns of coarse feldspar-bearing granodiorite (*R*1), tonalite porphyry (*R*2), tourmaline in quartz–tourmaline veins (T1, T2), and tourmaline-rich rock (T3, T4). Chondrite data from Taylor & McLennan (1985).

COMPOSITIONAL VARIATIONS

The average composition of tourmaline at Salikvan corresponds to $(Na_{0.53}Ca_{0.33})$ $(Mg_{1.75}Fe^{2+}_{0.91})$ $(Al_{5.59}Fe^{3+}_{0.42})$ $[Si_6O_{18}]$ (BO_3) $(OH,F)_4$. Tourmaline from this area generally has insufficient Al to fill the *Z* site. Tourmaline in quartz–tourmaline veins has greater *R*1 (Na + Ca) site occupancy (mean *R*1 = 0.90 *apfu*) and *R*3 (Al + 1.33*Ti) site occupancy (mean *R*3 = 5.77 *apfu*) than tourmaline in the tonalite porphyry (mean *R*1 = 0.88, mean *R*3 = 5.69 *apfu*) and in tourmaline-rich rocks along the contact between coarse granodiorite and the lower basic series. Tourmaline from the tonalite porphyry shows a higher *R*2 (Fe + Mg + Mn) site occupancy (mean *R*2 = 3.20 *apfu*) compared to tourmaline both in the quartz veins (mean *R*2 = 3.03 *apfu*) and tourmaline-rich rocks (mean *R*2 = 3.09 *apfu*). In general, tourmaline from tourmalinite has higher concentrations of Mg and lower Fe than tourmaline in tonalite porphyry and in quartz–tourmaline veins. The tourmaline from tourmaline-rich rocks has also higher Ca/(Ca + Na) values. In comparison, tourmaline in the tonalite porphyry displays lower Mg and higher Fe contents. Tourmaline in quartz–tourmaline veins lacks systematic compositional differences relative to the other types of tourmaline.

A plot of tourmaline compositions is given in Figure 8 in terms of Mg *versus* Fe. Compositional trends for different porphyry Cu–Mo deposits are shown for comparison. Magnesium is generally uniform between 1.50 and 2.00 *apfu*. The samples range from dravite to uvite; the slope of the regression between aluminum and iron has a correlation coefficient r of –0.88. Iron thus substitutes to a considerable extent for Al in the *R*3 site. Electron-microprobe traverses (Fig. 9) also indicate coupled Fe^{3+}–Al variations.

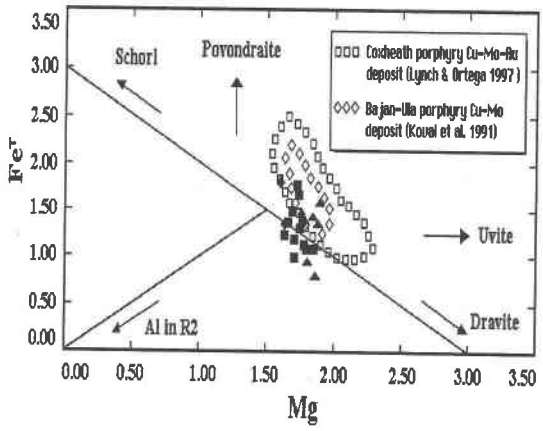

FIG. 8. Tourmaline compositions in terms of Fe^T *versus* Mg diagram. Chemical trends of tourmaline from other porphyry Cu–Mo deposits are plotted.

The chemical composition of tourmalines is shown on a tourmaline quadrilateral in Figure 10. The Ca content of the tourmalines from the Salikvan area ranges from 0.18 to 0.47 *apfu* and is correlated with the Fe/(Fe + Mg) value (correlation coefficient 0.74). An increase in the Ca content of tourmaline reflects the uvite substitution. Depending on the amount of magnesium in the *R*2 site, the excess iron occupies the *R*2 and *R*3 site. Thus, it gives rise to ferrous and ferric iron content in the tourmaline structure. The chemical composition of tourmaline samples from the Salikvan deposit on *R*1 + *R*2 *versus* *R*3 diagram (Fig. 11) presents a trend toward the uvite [Ca(Fe,Mg)](NaAl)$_{-1}$ end-member. Tourmaline from the quartz–tourmaline veins shows concentric zonation about the *c* axis (Fig. 9). Optical and compositional zoning were identified in tourmaline from quartz–tourmaline veins. Tourmaline with a light-colored core (Fig. 3B) has low Fe, Ca, Mg and Ti contents, but the Na and Al content in this type of tourmaline shows an increase toward the rim. Tourmaline with a dark core is richer in Mg, Ca, Fe and Ti, but depleted in Al and Na contents. Diverse patterns of chemical zoning in tourmaline indicate that distinct mineralizing events characterized by different hydrothermal processes played an important role in determining the compositions of tourmaline.

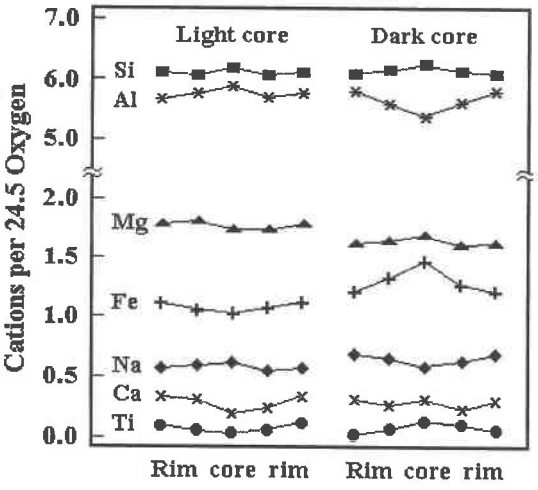

FIG. 9. Electron-microprobe traverses across zoned crystals of tourmaline from quartz–tourmaline veins.

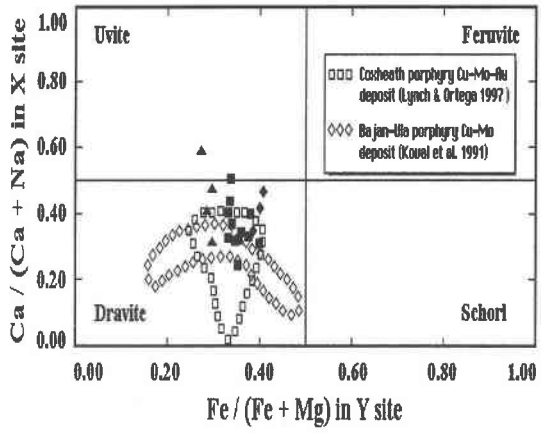

FIG. 10. Ca/(Ca + Na) at the *X* site *versus* Fe/(Fe + Mg) at the *Y* site of the tourmalines.

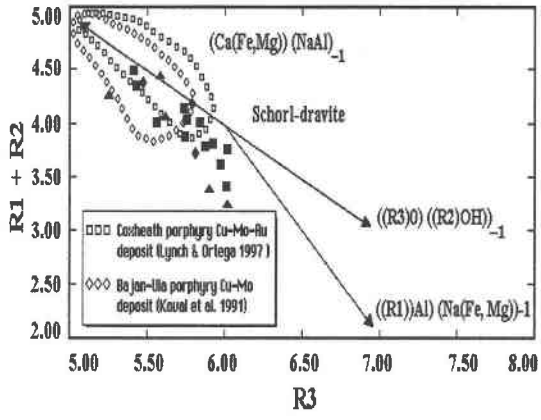

FIG. 11. Variation of (*R*1 + *R*2) *versus* *R*3 in tourmaline from the Salikvan porphyry Cu–Mo deposit. Data for tourmaline from various types of porphyry Cu–Mo deposits are shown for comparison.

Boron Isotope Studies

Boron isotope analyses were carried out on powdered pure separates of tourmaline from crushed tourmaline-rich rocks and quartz–tourmaline veins. The samples were dissolved in HF + HNO_3 acids with addition of mannitol in closed Teflon beakers (Nakamura *et al.* 1992), and the boron fractions were purified by cation-resin chemical columns and then analyzed using a negative-ion (BO^{2-}) thermal-ionization mass spectrometer (Swihart 1996). The $\delta^{11}B$ values (in ‰) are reported as $\delta^{11}B = [(^{11}B/^{10}B)_{sample} / (^{11}B/^{10}B)_{standard} - 1]*1000$. The boron standard is NIST boric acid SRM 951, prepared by the National Institute of Standards and Technology, Bethesda, Maryland. During the course of this study, about 20 analyses of this standard in the laboratory at Mainz have yielded an average $^{11}B/^{10}B$ value of $4.0090 \pm 0.7‰$ (2σ). Samples were analyzed with an average precision of the measurements better than $\pm 0.7‰$ (2σ).

A study of the isotopic composition of boron in tourmaline provides valuable information regarding the source of boron and the genesis of related mineralization. Boron isotope studies of tourmaline from hydrothermal ore deposits have largely focussed on massive sulfide deposits and tourmalinites (Palmer & Slack 1989, Slack *et al.* 1993). However, the number of other studies of boron isotopes on granite-related hydrothermal Sn–W, mesothermal Au, evaporites, and metamorphosed borate deposits has increased in recent years (Smith & Yardley 1996, Rowins *et al.* 1997, Palmer & Helvacı 1997, Jiang *et al.* 1997). Limited boron isotope data are available from granite-related hydrothermal deposits. In a study of tourmaline from a number of granite-related Sn–W veins, polymetallic deposits, and barren rocks in Nova Scotia, Clarke *et al.* (1989) reported $\delta^{11}B$ values of –18.5 to 3.5‰ with a low analytical precision (±7‰). Smith & Yardley (1996) analyzed tourmaline from the granite-related Sn deposits at Cornwall, southwestern England. They reported $\delta^{11}B$ values of –10.8 to –2.8‰ for tourmaline from hydrothermal veins and altered rocks; these show a similar range to that defined by tourmaline in granitic rocks (–12.7 to –5.9‰) and from tourmalinites (–10.5 to 0.7‰). Jiang & Palmer (1998) reported boron isotope data from granites and related hydrothermal metasomatic halos in the Guangxi tin province, southeastern China. They reported $\delta^{11}B$ value of –13.9‰ for tourmaline from granites, and –12.7 to –11.9‰ for tourmaline from greisen near granite in the Yidong granite-related tin deposit.

In the Salikvan deposit, tourmaline from a quartz–tourmaline vein has a $\delta^{11}B$ value of –9.4‰, whereas tourmaline from a tourmalinite has a similar $\delta^{11}B$ value, –9.0‰. The boron isotopic compositions of these samples fall within the $\delta^{11}B$ range of tourmaline from granite-related settings (Jiang & Palmer 1998). The boron isotope systematics indicate that the tourmaline grew during late-stage magmatic hydrothermal activity. Tourmaline from quartz–tourmaline veins has a higher content of Ag, Au, Pb, Sc, Sb, Mo, W, P, and Li than tourmaline from tourmaline-rich rocks (Table 2). However, tourmaline from quartz–tourmaline veins has lower contents of Mn, Ni, Co, and Cr than that from tourmalinite. Because of our limited boron isotope data on tourmaline, we are unable to establish correlations between trace-element contents and $\delta^{11}B$ values, but a decrease in Ag, Au, Pb, Sc, Sb, Mo, W, P, and Li contents accompanies an increase in $\delta^{11}B$ values.

Discussion

Trace-element variation in tourmaline

Trace-element data on tourmaline from a mineralized area may give important insights into the chemical characteristics and evolution of the hydrothermal system. Economic constraints and availability of tourmaline, however, restrict its practical application for geochemical exploration. Smith *et al.* (1987) discussed the use of trace-element geochemistry of tourmaline for certain districts on the basis of the widespread distribution of tourmaline in Mexican porphyry Cu–Mo deposits; in contrast, there is a lack of associated tourmaline in southwestern U.S. porphyry deposits. Tourmaline, in most of porphyry copper deposits, is found as an accessory mineral associated with potassic and phyllic alteration zones and hydrothermal breccias. In some porphyry copper deposits, tourmaline also accompanies late-stage sodic–calcic alteration subtypes.

In this study, the major, trace, and *REE* content of tourmaline from the weakly developed Salikvan porphyry Cu–Mo deposit is evaluated. Its major-element variations, together with that of tourmaline in other porphyry copper deposits, are discussed as an exploration guide for this style of mineralized systems. Tourmaline in the Salikvan deposit is found as an albite + tourmaline assemblage that is superimposed on the propylitic alteration zone. This formation reflects the mode of tourmaline occurrence developed at shallow depths.

Because of limited trace-element data on tourmaline from porphyry Cu–Mo deposits elsewhere, we are unable to make comparisons with our findings. Correlations between trace elements in tourmaline are categorized as excellent (*i.e.,* $r \geq 0.95$; Pb–Ag, Sb–Ag, V–Ag, V–Au, Sr–Ba, Cr–Co, W–P, V–P, Sb–Pb, V–Sb), very good (*i.e.,* $0.90 < r \leq 0.95$; Au–Ag, Li–Ag, P–Ag, W–Ag, Pb–Au, Mn–Cr, Zn–Cu, Mo–Li, Sb–Li, V–Li, Pb–Mo, Zr–Sn), good (*i.e.,* $0.80 < r \leq 0.90$; Mo–Ag, P–Au, Sb–Au, W–Au, Mn–Cu, Pb–Li, Sb–Mo, V–Mo, Sb–P, V–P, W–Sb, W–V), and moderate to good (*i.e.,* $0.70 < r \leq 0.80$; Li–Au, Mo–Au, Li–Ba, Pb–P, Sc–Pb, W–Pb). Correlations between trace elements in tourmaline indicate the similar geochemical behavior of these elements during tourmaline crystallization and later sodic alteration. Strong correlation coefficients between elements having similar ionic radii (*i.e.,* Pb–

Ag, Sr–Ba, Cr–Co) may hint at replacement during tourmalinization. Correlations involving pairs of elements with distinct ionic radii, however, may arise from both trace amounts of ore minerals trapped in the tourmaline and possible replacements in these minerals. A principal component analysis on 18 trace elements indicates that two components mainly are responsible for the variation according to lithology, mineralization and alteration processes, with 80.9% total variance. Principal component 1 is a strong association of P, Au, Ag, Sb, V, W, and Li, and a strong negative association of Mn, Co, and Cr, explaining 57.2% of the total variance in the data. Principal component 2 is a strong positive association of Ba and Sr, and a strong negative association of Zr and Sn, explaining 23.7% of the total variance in the data.

Variations in ferric and ferrous iron in tourmaline

The tourmaline from well-known porphyry Cu–Mo–Au deposits [*e.g.,* Bajan–Ula, Russia: Koval *et al.* (1991), Coxheath, Nova Scotia: Lynch & Ortega (1997)] is generally rich in ferric iron, suggesting that they are formed under relatively oxidizing hydrothermal conditions. The calculated ferric iron content of tourmaline-rich rocks is 0.53 *apfu* on average. The ferric iron content of tourmaline-rich rocks is higher than that of quartz–tourmaline veins (mean 0.36 *apfu*) and tonalite porphyry (mean 0.44 *apfu*). Calculated Fe^{3+}/Fe^{2+} values of tourmaline from Salikvan range from 0.04 to 1.92 (mean 0.51). The higher Fe^{3+}/Fe^{2+} values suggest that tourmalines in the Salikvan deposit formed under relatively oxidizing hydrothermal conditions. Tourmalines from the Bajan–Ula (Koval *et al.* 1991) and Coxheath porphyry Cu–Mo deposits (Lynch & Ortega 1997) also have higher Fe^{3+}/Fe^{2+} values in the range of 0.03 to 1.01 (mean 0.60) and 0.38 to 1.55 (mean 0.87), respectively. The interpretation that tourmalines from both of these deposits developed under relatively high $f(O_2)$ conditions agrees with the copper ± molybdenum metallogeny of the granitic rocks, which contain magnetite rather than ilmenite. Pirajno & Smithies (1992) proposed that the ratio FeO/(FeO + MgO) (*i.e.,* Fe#) of tourmaline can be a useful discriminant in distinguishing Sn–W deposits in terms of their distance from the granitic source. The tourmaline data are plotted on a Fe# *versus* MgO diagram (Fig. 12); we contend that the Salikvan deposit formed at shallow depths, possibly as a result of fluids that moved a long way from the main granitic source. This application of tourmaline composition is also in harmony with the field observation and microscopic studies. Most of amphiboles in the lower basic series and coarse granodiorite, especially at the top of the sequence in the study area, near Lake Karagöl, have been converted to tourmaline by hydrothermal fluids. Tourmaline-rich rocks (up to 5 cm thick) are observed at the contacts of these two lithologies. To convert amphibolite to tourmaline, Morgan & London (1989) demonstrated experimentally that an introduction of Al along with B (and local conservation of Fe and Mg) provide the most satisfactory conservation of mass and volume, and that Al in particular is soluble in B-rich aqueous fluids. Alteration of calcic amphibole to the tourmaline yielded the uvite component, especially in tourmaline-rich rocks. This type of substitution is observed in tonalite porphyry at the expense of plagioclase.

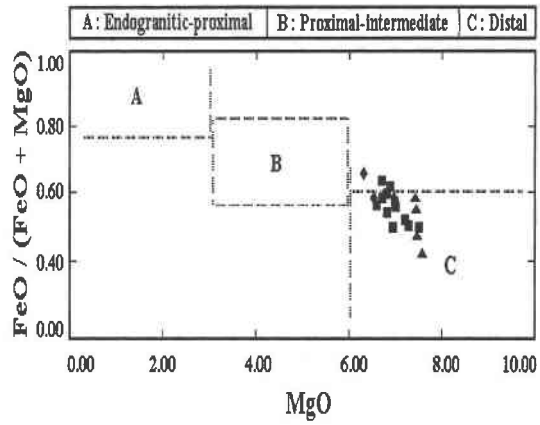

FIG. 12. FeO/(FeO + MgO) *versus* MgO of tourmaline from the Salikvan porphyry Cu–Mo deposit.

Chemical substitutions

Despite incomplete electron-microprobe data, tourmaline provides useful information about possible chemical substitutions during its crystallization. Different types of chemical substitutions in the *X*, *Y* and *Z* sites give rise to complex compositions (Foit & Rosenberg 1977, Henry & Guidotti 1985, Gallagher 1988, Burt 1989, Henry & Dutrow 1990). Aluminum-rich tourmaline generally contains enough Al to fill completely the *Z* site; excess Al is located in the *Y* site according to the $AlOMg_{-1}(OH)_{-1}$ and $\square AlNa_{-1}Mg_{-1}$ substitutions (Henry & Dutrow 1990). In lithium-poor aluminous tourmaline, calcium incorporation in the structure can be controlled by the dominant $CaMgO\square_{-1}Al_{-1}(OH)_{-1}$ substitution and, to a lesser extent, $CaMgNa_{-1}Mg_{-1}$ and $AlOMg_{-1}(OH)_{-1}$. Henry & Dutrow (1990) pointed out that in cases of $CaMgOM\square_{-1}Al_{-1}(OH)_{-1}$ as the dominant mechanism of substitution in aluminous tourmaline, there should be a general inverse correlation between Ca and *X*-site vacancies, and a poor correlation between Ca and Na. This substitution develops only in tourmaline in relatively aluminous bulk compositions, and is associated with significant *X*-site vacancies (Henry & Dutrow 1990). In the Salikvan tourmalines, (Na + Fe) is inversely correlated with Al ($r = -0.75$). The variation between Na and Ca with Al shows an inverse relationship, with $r = -0.54$. Electron-microprobe

results indicate that vacancies in the *X* site range up to 0.46 (mean 0.14), such that no significant *X*-site vacancies ($X_{total} < 0.50$) exist at Salikvan. Deficiencies in the *X* site show a positive correlation (r = 0.52) with Al in the *Z* site. A negative correlation (r = –0.69) between Fe^{2+} and Mg shows the existence of dravite and uvite components in the tourmaline. A plot of the data on the exchange-vector diagrams of Henry & Dutrow (1990) indicate that the Salikvan tourmaline contains the dominant substitutions $CaMgO\square_{-1}Al_{-1}(OH)_{-1}$, $CaMg\square_{-1}Al_{-2}$, and $CaMg_3OH\square_{-1}Al_{-3}O_{-1}$. There is an inverse relationship between Ca and vacancies in *X* site, with a correlation coefficient of r = –0.66 (Fig. 13A). On a Na* + Al* *versus* Ca + Mg* plot, tourmaline data from the Salikvan area yield a least-squares fit with a slope of –0.70 and correlation coefficient of r = –0.71 (Fig. 13B). No correlation (r = +0.008) exists between Ca and (Na + K) at the *X* site. These results indicate that $CaMgO\square_{-1}Al_{-1}(OH)_{-1}$ is the dominant mechanism for calcium incorporation in tourmaline from Salikvan. These variations are similar to those in the feruvite occurrences from footwall samples of the Sullivan Pb–Zn–Ag deposit in British Columbia. Jiang *et al.* (1996) attributed these variations to the dominant substitution vector $CaMgO\square_{-1}Al_{-1}(OH)_{-1}$ in the deep footwall samples of the Sullivan deposit. According to them, the Ca in feruvite also diminishes *X*-site vacancies. It seems that calcium-rich plagioclase and calcic amphiboles have controlled the incorporation of Ca into the Salikvan tourmalines and thus yielded the uvite instead of the feruvite component.

Conclusions

1. Tourmaline from the Salikvan porphyry Cu–Mo deposit is identified in three main types: (i) quartz–tourmaline veins, (ii) tonalite porphyry, and (iii) tourmaline-rich metasomatic rocks.

2. The chemical composition of tourmaline is dominantly dravitic and, to a lesser extent, there is a uvite component. The uvite component formed by the reaction of Fe-rich hydrothermal fluids with Ca-rich amphibole and plagioclase in the magmatic host-rocks.

3. The tourmaline from quartz–tourmaline veins has higher levels of Pb, Zn, Ag, Sr, Sb, Ba, W, P, Sn, P, Li, and Au, but lower levels of Ni, Co, Mn, Cr and Zr than the tourmaline from tourmaline-rich rocks. According to correlation studies between trace elements in tourmaline, there are similar patterns of geochemical behavior during tourmaline crystallization and later processes of alteration.

4. The tourmaline from Salikvan is generally rich in ferric iron, as is the tourmaline from other porphyry Cu–Mo–Au deposits in the world. The calculated Fe^{3+}:Fe^{2+} ratio of the tourmaline reflects the relatively oxidizing hydrothermal conditions of crystallization.

5. Chemical substitution in tourmaline of the Salikvan suite involves the exchange vector $CaMgO\square_{-1}Al_{-1}(OH)_{-1}$.

6. Boron isotope compositions of tourmalines point out the granite-related tourmaline settings and source of the boron in the late-magmatic hydrothermal fluids.

7. Chondrite-normalized patterns of *REE* are poorly fractionated, with general decrease in light *REE* and increase in *HREE*.

8. Concentric zonation, with a light and dark pleochroic schemes at the core of crystals, indicates that compositionally different hydrothermal fluids are responsible for the development of tourmaline.

Acknowledgements

We especially thank J.F. Slack for encouraging us in this study. The text has greatly benefitted from the critical reviews and comments by J.F. Slack, R.F. Martin, and G. Lynch. We are also grateful to A. Özcan for valu-

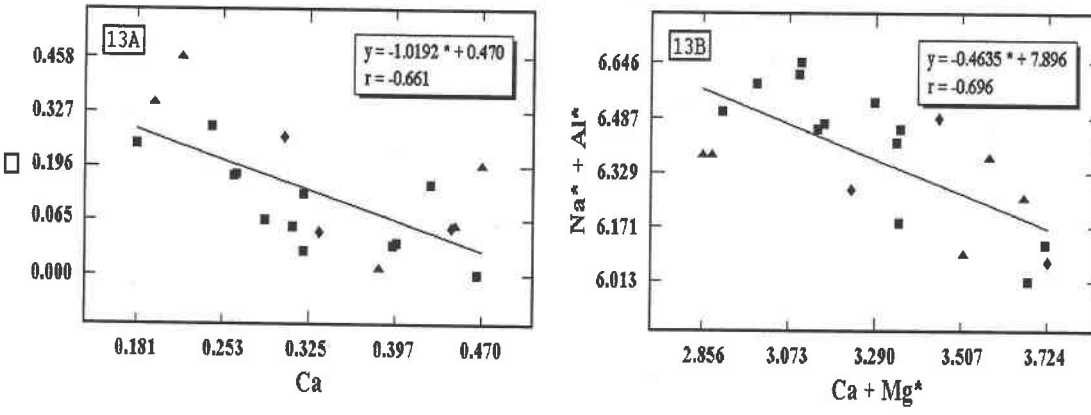

FIG. 13. A. *X*-site vacancies (□) *versus* Ca at the *X* site. B. Na* + Al* *versus* Ca + Mg* for tourmaline from the Salikvan area, where Na* = Na + K, Al* = Al + 2Ti, Mg* = Mg + Fe + Mn – Ti.

able assistance during operation of the electron-microprobe at the Şişecam, and to M. Budakoglu for sample preparation.

References

ASLANER, M., VAN, A. & YALÇINALP, B. (1995): General features of Pontide metallogenic belt. *In* Proc. Int. Symp. on the Geology of the Black Sea Region (A. Erler, T. Ercan, E. Bingöl & S. Örçen, eds.). General Directorate of Mineral Research and Exploration and Chamber of Geological Engineers, Ankara, Turkey (209-213).

BURT, D.M. (1989): Vector representation of tourmaline compositions. *Am. Mineral.* **74**, 826-839.

CAMUS, F. (1975): Geology of the El Teniente orebody with emphasis on wall-rock alteration. *Econ. Geol.* **70**, 1341-1372.

CARTEN, R.B. (1986): Sodium–calcium metasomatism: chemical, temporal, and spatial relationships at the Yerington, Nevada, porphyry copper deposit. *Econ. Geol.* **81**, 1495-1519.

CLARKE, D.B., REARDON, N.C., CHATTERJEE, A.K. & GREGOIRE, D.C. (1989): Tourmaline composition as a guide to mineral exploration: a reconnaissance study from Nova Scotia using discriminant function analysis. *Econ. Geol.* **84**, 1921-1935.

CLELAND, J. M., MOREY, G. B. & MCSWIGGEN, P. L. (1996): Significance of tourmaline-rich rocks in the North Range Group of the Cuyuna Iron Range, east-central Minnesota. *Econ. Geol.* **91**, 1282- 1291.

FARMER, C.B. & HALLS, C. (1993): Petrogenetic evolution of cassiterite-bearing lodes at South Crofty mine, Cornwall, United Kingdom. *In* Proc. 8th Quad. IAGOD Symp. (Y. T. Maurice, ed.). E. Schweizerbart'sche Verlagsbuchhandlung, Stuttgart, Germany (365-381).

FOIT, F.F., JR. & ROSENBERG, P.E. (1977): Coupled substitutions in the tourmaline group. *Contrib. Mineral. Petrol.* **62**, 109-127.

GALLAGHER, V. (1988): Coupled substitutions in schorl–dravite tourmaline: new evidence from SE Ireland. *Mineral. Mag.* **52**, 637-650.

GARBA, I. (1996): Tourmalinization related to Late Proterozoic – early Paleozoic lode gold mineralization in the Bin Yauri area, Nigeria. *Mineral. Deposita* **31**, 201-209.

GORELIKOVA, N.V. & NAUMOVA, V.V. (1987): Trace-element parageneses in tourmaline as indicators of zoning and productivity of tin mineralization. *Dokl. Acad. Sci. USSR, Earth Sci. Sect.* **297**, 179-183.

GRIFFIN, W.L., SLACK, J.F., RAMSDEN, A.R., WIN, TIN-TIN & RYAN, C.G. (1996): Trace elements in tourmalines from massive sulfide deposits and tourmalinites: geochemical controls and exploration applications. *Econ. Geol.* **91**, 657-675.

HELLINGWERF, R.H., GATEDAL, K., GALLAGHER, V. & BAKER, J.H. (1994): Tourmaline in the central Swedish ore district. *Mineral. Deposita* **29**, 189-205.

HENRY, D.J. & DUTROW, B.L. (1990): Ca substitution in Li-poor aluminous tourmaline. *Can. Mineral.* **28**, 111-124.

_____ & GUIDOTTI, C.V. (1985): Tourmaline as a petrogenetic indicator mineral: an example from the staurolite-grade metapelites of NW Maine. *Am. Mineral.* **70**, 1-15.

JIANG, SHAO-YONG & PALMER, M.R. (1995): Trace and rare-earth elements in tourmaline from hydrothermal deposits and their genetic significance. *Terra Nova* **7**, *Abstr. Suppl.* **1**, 211.

_____ & _____ (1998): Boron isotope systematics of tourmaline from granites and pegmatites: a synthesis. *Eur. J. Mineral.* **10**, 1253-1265.

_____, _____, MCDONALD, A.M., SLACK, J.F. & LEITCH, C.H.B. (1996): Feruvite from the Sullivan Pb–Zn–Ag deposit, British Columbia. *Can. Mineral.* **34**, 733-740.

_____, _____, PENG, Q.-M. & YANG, JING-HONG (1997): Chemical and stable isotopic compositions of Proterozoic metamorphosed evaporites and associated tourmalines from the Houxianyu borate deposit, eastern Liaoning, China. *Chem. Geol.* **135**, 189-211.

KAHRAMAN, I., ÇAĞLAR, O., SATIR, F., ÇAKIR, M., YILMAZ, T., TÜRKMEN, I. & KARANIS, H.A. (1987): A preliminary geological and mineralization study of Rize–Fındıklı, Artvin – Arhavi – Hopa – Yusufeli (north) regions. *MTA Rep.* **JD-510** (in Turkish).

KAMITANI, M., OKABE, K. & BEKTAŞ, O. (1977): A preliminary report on copper and molybdenum occurrences in northeast Turkey, Artvin, Yüksekoba regions. *MTA Rep.* **1523** (in Turkish).

_____ & TAKAOĞLU, S. (1976): Copper and molybdenum occurrences in Artvin – Yusufeli – Balcılı area. *MTA Rep.* **1396** (in Turkish).

KING, R.W. (1988): Geochemical characteristics of tourmaline from Superior province Arhean lode gold deposits: implications for source regions and processes. *Bicentennial Gold '88, Geol. Soc. Aust., Abstr. Ser.* **23**, 445-447.

_____ & KERRICH, R.W. (1986): Tourmaline in Archean lode gold deposits. II. REE distribution and Sr isotope characteristics. *Geol. Soc. Am., Abstr. Programs* **18**, 657.

_____, _____ & DADDAR, R. (1988): REE distributions in tourmaline: an INAA technique involving pretreatment by B volatilization. *Am. Mineral.* **73**, 424-431.

KITAYEV, N.A. & BOGATYREV, P.V. (1984): Tourmaline from gold ore deposits. *Dokl. Acad. Sci. USSR, Earth Sci. Sect.* **274**, 164-166.

KLEIN, C. & BEUKES, N.J. (1989): Geochemistry and sedimentology of a facies transition from limestone to iron-formation deposition in the Early Proterozoic Transvaal Supergroup, South Africa. *Econ. Geol.* **84**, 1733-1774.

KOVAL, P.V., ZORINA, L.D., KITAJEV, N.A., SPIRIDONOV, A.M. & ARIUNBILEG, S. (1991): The use of tourmaline in geochemical prospecting for gold and copper mineralization. *J. Geochem. Explor.* **40**, 349-360.

LAYNE, G.D. & SPOONER, E.T.C. (1991): The JC tin skarn deposit, southern Yukon Territory. 1. Geology, paragenesis, and fluid inclusion microthermometry. *Econ. Geol.* **86**, 29-47.

LONDON, D. & MANNING, D.A.C. (1995): Chemical variation and significance of tourmaline from southwest England. *Econ. Geol.* **90**, 495-519.

LUBIS, H., PRIHATMOKO, S. & JAMES, L.P. (1994): Bulagidun prospect: a copper, gold and tourmaline bearing porphyry and breccia system in northern Sulawesi, Indonesia. *J. Geochem. Explor.* **50**, 257-278.

LYNCH, J.V.G. (1989): Hydrothermal alteration, veining, and fluid inclusion characteristics of the Kalzas wolframite deposit, Yukon. *Can. J. Earth Sci.* **26**, 2106-2115.

_____ & ORTEGA, J. (1997): Hydrothermal alteration and tourmaline–albite equilibria at the Coxheath porphyry Cu–Mo–Au deposit, Nova Scotia. *Can. Mineral.* **35**, 79-94.

MAO, JINGWEN (1995): Tourmalinite from northern Guangxi, China. *Mineral. Deposita* **30**, 235-245.

MITTWEDE, S.K., HELVACI, C. & KARAMANDERESI, I.H. (1995a): Geochemistry, exploration significance, and genesis of tourmalinites from the Lake Bafa, southwestern Anatolia, Turkey. *Int. Earth Sci. Colloquium on the Aegean Region*, 40.

_____, SINCLAIR, W.D., HELVACI, C. & KARAMANDERESI, I.H. (1995b): Geochemistry of quartz–tourmaline nodules from Irmadan (Muğla–Yatağan), Türkiye. *Second Int. Turkish Geol. Workshop*, 74.

MOORE, W. J., MCKEE, E. H. & AKINCI, Ö. (1986): Chemistry and chronology of plutonic rocks in the Pontide mountains, northern Turkey. *In* European Copper Deposits (S. Jankovic & R.H. Sillitoe, eds.). Faculty of Geology and Mining, Belgrade University, Belgrade, Yugoslavia (209-215).

MORGAN, G.B., VI & LONDON, D. (1989): Experimental reactions of amphibolite with boron-bearing aqueous fluids at 200 MPa: implications for tourmaline stability and partial melting in mafic rocks. *Contrib. Mineral. Petrol.* **102**, 281-297.

NAKAMURA, E., ISHIKAWA, T., BIRCK, J.-L. & ALLÈGRE, C.J. (1992): Precise boron isotopic analysis of natural rock samples using a boron–mannitol complex. *Chem. Geol. (Isotope Geosci. Sect.)* **94**, 193-204.

PALMER, M.R. & HELVACI, C. (1997): The boron isotope geochemistry of the Neogene borate deposits of western Turkey. *Geochim. Cosmochim. Acta* **61**, 3161-3169.

_____ & SLACK, J.F. (1989): Boron isotopic composition of tourmaline from massive sulfide deposits and tourmalinites. *Contrib. Mineral. Petrol.* **103**, 434-451.

PATTERSON, D.J., OHMOTO, H. & SOLOMON, M. (1981): Geologic setting and genesis of cassiterite–sulfide mineralization at Renison Bell, western Tasmania. *Econ. Geol.* **76**, 393-438.

PIRAJNO, F., PETZEL, V.F.W. & JACOB, R.E. (1987): Geology and alteration–mineralization of the Brandberg West Sn–W deposit, Damara Orogen, South West Africa/Namibia. *Trans. Geol. Soc. S. Afr.* **90**, 256-269.

_____ & SMITHIES, R.H. (1992): The FeO/(FeO + MgO) ratio of tourmaline: a useful indicator of spatial variations in granite-related hydrothermal mineral deposits. *J. Geochem. Explor.* **42**, 371- 381.

ROWINS, S.M., GROVES, D.I., MCNAUGHTON, N.J., PALMER, M.R. & ELDRIDGE, C.S. (1997): A reinterpretation of the role of granitoids in the genesis of Neoproterozoic gold mineralization in the Telfer Dome, western Australia. *Econ. Geol.* **92**, 133-160.

SILLITOE, R.H. (1973): Geology of the Los Pelambres porphyry copper deposit, Chile. *Econ. Geol.* **68**, 1-10.

_____ & SAWKINS, F.J. (1971): Geologic, mineralogic and fluid inclusion studies relating to the origin of copper-bearing tourmaline breccia pipes, Chile. *Econ. Geol.* **66**, 1028-1041.

SKEWES, M.A. (1992): *Miocene and Pliocene Copper-Rich Breccias from the Andes of Central Chile (32°–34°S).* Ph.D. thesis, Univ. of Colorado, Boulder, Colorado.

SLACK, J.F. (1996): Tourmaline associations with hydrothermal ore deposits. *In* Boron: Mineralogy, Petrology, and Geochemistry (E.S. Grew & L.M. Anovitz, eds.). *Rev. Mineral.* **33**, 559-643.

_____, PALMER, M.R., STEVENS, B.P.J. & BARNES, R.G. (1993): Origin and significance of tourrmaline-rich rocks in the Broken Hill district, Australia. *Econ. Geol.* **88**, 505-541.

SMITH, M.P. & YARDLEY, B.W.D. (1996): The boron isotopic composition of tourmaline as a guide to fluid processes in the southwestern England orefield: an ion microprobe study. *Geochim. Cosmochim. Acta* **60**, 1415-1427.

SMITH, S.M., CLOSS, L.G. & THEOBALD, P.K. (1987): Trace element variation in hydrothermal tourmalines associated with mineralization: El Correo, Sonora, Mexico. *In* GEOXPO/86: Exploration in the North American Cordillera (I.L. Elliot & B.W. Smee, eds.). Association of Exploration Geochemists, Calgary, Alberta (109-125).

SWIHART, G.H. (1996): Instrumental techniques for boron isotope analysis. *In* Boron: Mineralogy, Petrology, and Geochemistry (E.S. Grew & L.M. Anovitz, eds.). *Rev. Mineral.* **33**, 845-862.

TAYLOR, S.R. & MCLENNAN, S.M. (1985): *The Continental Crust: its Composition and Evolution.* Blackwell, London, U.K.

TOKEL, S. (1995): Magmatic and geochemical evolution of the Pontide segment of the northern Tethys subduction system. *In* Proc. Int. Symp. on the Geology of the Black Sea Region (A. Erler, T. Ercan, E. Bingöl & S. Örçen, eds.). General Directorate of Mineral Research and Exploration and Chamber of Geological Engineers, Ankara, Turkey (163-170).

WARNAARS, F.W., HOLMGGREN, C.D. & BARASSI, S.F. (1985): Porphyry copper and tourmaline breccias at Los Bronces – Rio Blanco, Chile. *Econ. Geol.* **80**, 1544-1565.

WRIGHT, J.H. & KWAK, T.A.P. (1989): Tin-bearing greisens of Mount Bischoff, northwestern Tasmania, Australia. *Econ. Geol.* **84**, 551-574.

YAVUZ, F. (1992): *The Genetic Investigation of Balcılı (Artvin) and Güzelyayla (Trabzon) Copper–Molybdenum Occurrences in the Metallogenic Province of Eastern Pontide.* Ph.D. thesis, Istanbul Technical Univ., Istanbul, Turkey (in Turkish).

_____ (1997): TOURMAL: software package for tourmaline, tourmaline-rich rocks and related ore deposits. *Comput. & Geosci.* **23**, 947-959.

_____ & BÜRKÜT, Y. (1993): Petrology of the Balcılı (Artvin) granitoids from the calc-alkali province of northeast Turkey. *Terra Nova* **5** (*Abst. Suppl.* **1**), 540.

_____ & ÖZTAŞ, T. (1997): BIOTERM – a program for evaluating and plotting microprobe analyses of biotite from barren and mineralized magmatic suites. *Comput. & Geosci.* **23**, 897-907.

Received June 18, 1998, revised manuscript accepted May 30, 1999.